Synthesis and structures of crystalline solvates formed of pyridinium *N*-phenoxide (Reichardt's-type) betaine dyes and alcohols†

Sandra Kurjatschij, Wilhelm Seichter and Edwin Weber*

Received (in Montpellier, France) 7th October 2009, Accepted 1st February 2010
First published as an Advance Article on the web 14th April 2010
DOI: 10.1039/b9nj00540d

Four new betaine dyes of the Reichardt's type featuring two tolyl substituents in different attachment (**2–4**) or being an analogous 1-naphthyl derivative (**5**) have been synthesized and described with reference to their negative solvatochromism. The dinaphthyl derivative **5** and also a corresponding intermediate nitrophenol **9d** were shown with variable-temperature NMR spectroscopy to form conformational atropisomers in solution. Crystal structures of seven alcoholic solvent complexes including the unsubstituted parent compound (**1**) and different alcohols [**1**·EtOH (1 : 1), **1**·*i*-PrOH (1 : 1), **2**·MeOH (1 : 2), **3**·*i*-PrOH (1 : 1), **3**·*n*-BuOH (1 : 1), **4**·EtOH (1 : 2) and **5**·MeOH (1 : 3)] have been studied using X-ray diffraction methods. The betaine dyes exist as genuine zwitterion ground state structures in the solid state with twisted conformation between the phenoxide and pyridinium rings. With the exception of **3a** [**3**·*i*-PrOH (1 : 1)], the alcohol guests in the complexes are hydrogen bonded to the oxygen atom of the phenoxide units, whereas in the *i*-PrOH complex of **3**, the alcohol forms trimeric clusters without specific interaction with the betaine framework. From the packing modes in the crystals, the solvated betaines may be classified either as co-ordination type inclusion compounds with pocket-like host arrangements [**1**·EtOH (1 : 1), **1**·*i*-PrOH (1 : 1), **2**·MeOH (1 : 2), **3**·*n*-BuOH (1 : 1), **4**·EtOH (1 : 2) and **5**·MeOH (1 : 3)], or a true clathrate with channel-type topology [**3**·*i*-PrOH (1 : 1)].

Introduction

Pyridinium *N*-phenoxide betaine dyes, commonly known as the Reichardt's type dyes,[1] are of great interest due to the phenomena of solvatochromism, thermochromism, piezochromism, and halochromism.[2] That is, the position of their longest wavelength intermolecular charge-transfer absorption band of their UV-vis absorption spectra depends on solvent polarity, solution temperature, external pressure, and on the nature and concentration of added salts.[3] The standard pyridinium *N*-phenoxide betaine dye **1** (Scheme 1) exhibiting extraordinarily large negative solvatochromism has been used to set up an empirical scale of solvent polarity [$E_T(30)$ values][4,5] to probe micellar environments[6] and to determine the composition of binary solvent mixtures[7] including the amount of water in organic solvents.[8] Moreover, chemical sensor development[9] and other materials' design[10,11] have taken advantage of the particular behavior of the betaine dyes.

This has stimulated the synthesis of a large number of different pyridinium *N*-phenoxide betaine dyes with special and improved properties.[3,5,12,14] Nevertheless, solid state structures of the Reichardt's type dyes have only scarcely been investigated, except for the early X-ray crystal structure determination of a bromo-substituted derivative of the parent betaine dye **1** as an ethanol solvate,[15] a recent structure of the hydrate of a substituted derivative of **1**[16] and of a related *ortho*-betaine.[12] A number of pyridinium salts of the Reichardt's compounds formed with different acids, in some cases containing solvent molecules in the crystal lattice, have also been

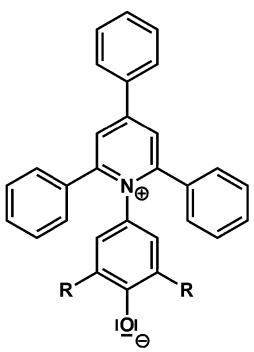

1 R = C_6H_5
2 R = 2-$C_6H_4CH_3$
3 R = 3-$C_6H_4CH_3$
4 R = 4-$C_6H_4CH_3$
5 R = 1-Naphthyl

1a **1** • EtOH (1:1)
1b **1** • *i*-PrOH (1:1)
2a **2** • MeOH (1:2)
3a **3** • *i*-PrOH (1:1)
3b **3** • BuOH (1:1)
4a **4** • EtOH (1:2)
5a **5** • MeOH (1:3)

Scheme 1 Betaine dyes and solvent complexes studied.

Institut für Organische Chemie, Technische Universität Bergakademie Freiberg, Leipziger Str. 29, D-09596 Freiberg/Sachsen, Germany. E-mail: edwin.weber@chemie.tu-freiberg.de; Fax: +49 (0) 37 31-39 31 70

† CCDC reference numbers 746916–746922. For crystallographic data in CIF or other electronic format see DOI: 10.1039/b9nj00540d

reported,[17–20] but they do not really feature the typical betaine structure under discussion here. Similar relations have recently been shown for the crystalline complexes of several other betaines.[21–24] Remarkably, the known crystal structures of the Reichardt's type betaines demonstrate twisted conformations of the π-systems, thus giving rise to impairment of the conjugation and asking for more details of structural studies. Moreover, discovering the modes of supramolecular contacts[25–27] between the betaine dye and interacting solvent molecules is another interesting target.

In the current work, we describe the synthesis of the new betaine dyes **2–5** (Scheme 1) and report on the X-ray structures of seven crystalline solvent complexes that involve the betaine dyes **1–5** with different alcohols included in the crystal lattice, *i.e.* **1a** [**1**·EtOH (1 : 1)], **1b** [**1**·*i*-PrOH (1 : 1)], **2a** [**2**·MeOH (1 : 2), **3a** [**3**·*i*-PrOH (1 : 1)], **3b** [**3**·*n*-BuOH (1 : 1)], **4a** [**4**·EtOH (1 : 2)], and **5a** [**5**·MeOH (1 : 3)]. We report also on the stereoisomerism of the dinaphthyl-substituted betaine **5** and the corresponding *p*-nitrophenol intermediate **9d** based on variable temperature NMR studies, giving information on the rotational barriers in these molecules.

Results and discussion

Synthesis

The synthesis of the new Reichardt's type betaine dyes **2–5** (Scheme 2) was accomplished following on principle the established procedures for the preparation of *para*-pyridinium *N*-phenoxides.[4,28,29] Here, the respective 2,6-diaryl-substituted 4-aminophenols **10a–d**, obtained by hydrogenation of the corresponding nitrophenols **9a–d**, were condensed with 2,4,6-triphenylpyrylium hydrogen sulfate (**11**) in the presence of sodium acetate to give, on addition of sodium hydroxide, the respective betaines. The nitrophenols **9a–d** were obtained by condensation reaction between 2-nitromalonaldehyde-Na (**8**) and the corresponding 1,3-diaryl-substituted propan-2-ones **7a–d**.[30] The ketones **7a–d** were synthesized from **6a–d** using two alternative literature procedures specified as A[31] and B[32] in Scheme 2. Process A involves a historical solid state distillation of the calcium salts of the correspondingly aryl-substituted acetic acids, while the more recently developed process B represents a reaction of the respective arylacetic acid with *N*,*N*-dicyclohexylcarbodiimide (DCC) catalyzed by 4-*N*,*N*-dimethylaminopyridine (4-DMAP). The yields obtained are moderate but were found higher in the case of B (Scheme 2).

Reichardt's type betaines were shown to crystallize as hydrates[14,16,28,29] or containing another solvent of crystallization.[15] This is also a characteristic feature of the betaines **2–5** being isolated as hydrates or stoichiometric complexes with alcohols (MeOH, EtOH, *i*-PrOH, *n*-BuOH) on crystallization from these solvents. Representative complexes (Scheme 1) have been studied in view of their X-ray crystal structures that are discussed below.

X-ray structural studies

Crystal data for **1a** [**1**·EtOH (1 : 1)], **1b** [**1**·*i*-PrOH (1 : 1)], **2a** [**2**·MeOH (1 : 2), **3a** [**3**·*i*-PrOH (1 : 1)], **3b** [**3**·*n*-BuOH (1 : 1)], **4a** [**4**·EtOH (1 : 2)] and **5a** [**5**·MeOH (1 : 3)] are given in Table 1. Structural features of the betaine dye molecules, including torsion angles and selected bond lengths, are shown in Table 2. Geometric parameters of possible intermolecular hydrogen bond interactions are presented in Table 3. The solvent molecules in **3a** and **3b**, as well as one of the ethanol molecules in **4a**, are disordered and turned out to be difficult to refine. In order to gain reasonable molecular geometries, bond lengths were restrained to ideal values.

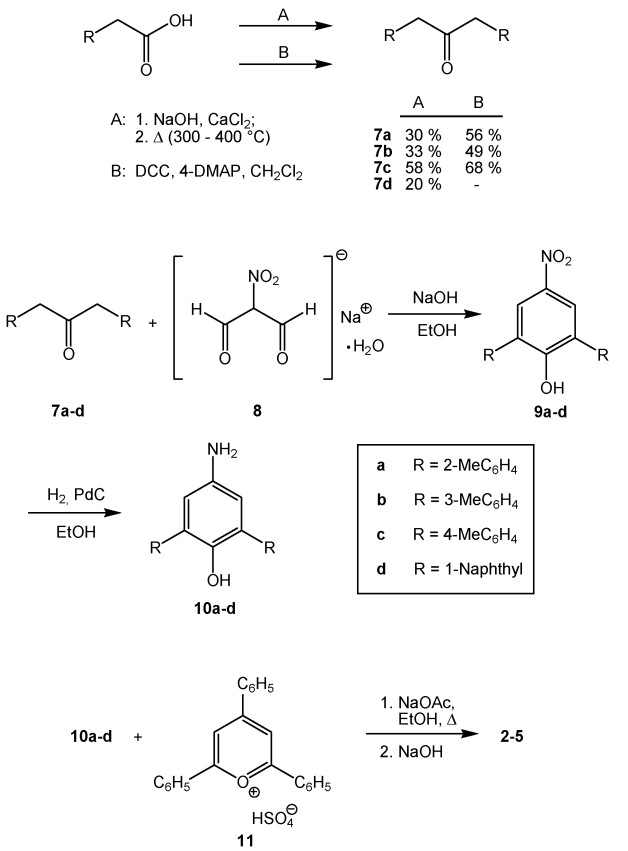

Scheme 2 Reaction scheme for the synthesis of the betaine dyes **2–5**.

The conformation of the betaine dye molecules **1–5** in their solvate structures can be described by a set of six torsion angles, denoted as τ_1–τ_6 in Scheme 3 (Table 2). In this connection, particular interest focuses on the conformational features that involve the molecular fragment given by the rings *I* and *II*, which are of opposite electronic nature. The bond distances in the molecules are in good agreement with those found in the crystal structures of related compounds.[15,16] A detailed analysis reveals that the C–O bonds of the betaines are significantly shortened in comparison with those of the protonated derivatives (phenolic pyridinium salts)[18–20] [1.268(3)–1.307(4) *vs.*1.336–1.364 Å], whereas the C–N bond length between the aromatic rings *I* and *II* (Scheme 3) seems to be less affected by deprotonation of the phenolic group. The contraction of the C–O bond and the elongation of the neighbouring C–C bonds indicate a partial quinoid character of the phenolate ring. The pyridinium and the phenolate rings are not co-planar, but twisted. The dihedral angle formed by their ring planes ranges between 55.2(1) and 74.6(2)°.

Table 1 Crystallographic and structure refinement data of the compounds studied

Compound	1a	1b	2a	3a	3b	4a	5a
Empirical formula	$C_{41}H_{29}NO\cdot C_2H_6O$	$C_{41}H_{29}NO\cdot C_3H_8O$	$C_{43}H_{33}NO\cdot 2\ CH_4O$	$C_{43}H_{33}NO\cdot C_3H_8O$	$C_{43}H_{33}NO\cdot C_4H_{10}O$	$C_{43}H_{33}NO\cdot 2\ C_2H_6O$	$C_{49}H_{33}NO\cdot 3\ CH_4O$
Formula weight	597.72	611.75	643.79	639.80	653.82	671.84	747.89
Colour	Bluish-violet	Blue	Redish-violet	Blue	Blue	Bluish-violet	Redish-violet
Crystal system	Monoclinic	Monoclinic	Monoclinic	Rhombohedral	Monoclinic	Monoclinic	Monoclinic
Space group	$P2_1/n$	$P2_1/n$	$P2_1/c$	$R\bar{3}c$	$P2_1/c$	$P2_1/n$	$P2_1/c$
a/Å	10.1428(3)	10.4500(7)	10.8713(2)	18.822(1)	8.8952(2)	11.9196(3)	13.2600(5)
b/Å	19.0295(6)	19.7456(11)	16.8352(4)	18.822(1)	18.8888(3)	19.0346(4)	17.3132(6)
c/Å	17.0312(5)	16.6334(9)	18.9751(4)	18.822(1)	21.0329(4)	16.6949(5)	18.2974(6)
α (°)	90.0	90.0	90.0	104.15(1)	90.0	90.0	90.0
β (°)	102.607(2)	105.934(3)	92.713(1)	104.15(1)	90.084(1)	98.110(1)	104.518(2)
γ (°)	90.0	90.0	90.0	104.15(1)	90.0	90.0	90.0
V/Å^3	3207.98(17)	3300.3(3)	3468.94(13)	5932.3(5)	3533.94(12)	3749.94(17)	4066.5(3)
Z	4	4	4	6	4	4	4
$V(000)$	1264	1296	1368	2040	1392	1432	1584
V_c/mg m^{-3})	1.238	1.231	1.233	1.075	1.229	1.190	1.222
μ/mm^{-1}	0.075	0.074	0.076	0.500	0.074	0.073	0.076
Data collection							
T/K	90(2)	90(2)	93(2)	193(2)	123(2)	123(2)	90(2)
No. of collected reflections	41306	22167	32121	10111	87340	39398	34681
Within the θ-limit (°)	1.6–29.1	1.6–26.4	1.6–26.4	3.0–65.0	1.4–29.1	1.6–29.1	1.6–26.4
Index ranges $\pm h$, $\pm k$, $\pm l$	−13/13, −26/18, −23/23	−12/6, −24/24, −20/20	−13/13, −14/20, −23/23	−20/22, −22/0, −13/17	−12/12, −25/25, −28/28	−16/16, −23/26, −22/22	−16/16, −21/21, −22/21
No. of unique reflections	8560	6492	6979	3361	9491	10055	8347
R_{int}	0.0354	0.0737	0.0301	0.0566	0.0424	0.0264	0.0519
Refinement calculations: full-matrix least-squares on all F^2 values							
Weighting expression w[a]	$[\sigma^2(F_o^2) + (0.0815P)^2 + 1.3308P)^{-1}$	$[\sigma^2(F_o^2) + (0.0866P)^2 + 1.4188P)^{-1}$	$[\sigma^2(F_o^2) + (0.0637P)^2 + 3.6573P)^{-1}$	$[\sigma^2(F_o^2) + (0.1303P)^2 + 0.6070P)^{-1}$	$[\sigma^2(F_o^2) + (0.0811P)^2 + 1.8362P)^{-1}$	$[\sigma^2(F_o^2) + (0.0826P)^2 + 1.9646P)^{-1}$	$[\sigma^2(F_o^2) + (0.0999P)^2 + 6.8573P)^{-1}$
No. of refined parameters	417	429	453	226	471	482	521
No. of F values used [$I > 2\sigma(I)$]	6809	4183	5347	2119	7056	7371	5324
Final R-Indices							
$R(= \Sigma\|\Delta F\|/\Sigma\|F_o\|)$	0.0471	0.0549	0.0508	0.0559	0.0495	0.0520	0.0717
wR on F^2	0.1538	0.1859	0.1499	0.1882	0.1623	0.1656	0.2407
S (= goodness of fit on F^2)	1.100	1.054	1.092	1.015	1.070	1.036	1.052
Final $\Delta\rho_{max}/\Delta\rho_{min}$/e Å^{-3}	0.38/−0.35	0.38/−0.30	0.49/−0.41	0.42/−0.29	0.49/−0.44	0.37/−0.38	0.56/−0.42

[a] $P = (F_o^2 + 2F_c^2)/3$.

Table 2 Relevant conformational parameters of the compounds studied

Compound	1a	1b	2a	3a	3b	4a	5a
Torsion angles[a]							
τ_1	64.8(2)	58.8(3)	69.3(2)	55.2(1)	66.4(2)	74.6(2)	63.9(4)
τ_2	−18.8(2)	−19.9(4)	19.9(3)	−32.5(2)	−13.4(2)	−19.4(2)	5.8(5)
τ_3	−32.4(2)	−33.2(3)	69.8(3)	−78.8(3)	34.9(2)	41.6(2)	−73.5(4)
τ_4	36.4(2)	36.4(3)	−55.6(3)	−78.8(3)	−31.7(2)	−31.7(2)	−61.8(4)
τ_5	37.2(2)	41.6(3)	42.2(3)	50.4(3)	38.2(2)	56.2(2)	49.7(4)
τ_6	51.0(2)	53.6(3)	57.4(3)	50.4(3)	59.3(2)	71.2(2)	54.3(4)
Bond lengths							
C(1)–O(1)	1.279(2)	1.278(3)	1.288(2)	1.268(3)	1.280(2)	1.290(2)	1.307(4)
C(1)–C(2)	1.453(2)	1.451(3)	1.437(3)	1.438(2)	1.450(2)	1.441(2)	1.431(4)
C(2)–C(3)	1.389(2)	1.387(3)	1.386(3)	1.382(3)	1.389(2)	1.389(2)	1.391(4)
C(3)–C(4)	1.385(2)	1.395(3)	1.390(3)	1.377(2)	1.387(2)	1.383(2)	1.389(4)
C(4)–C(5)	1.386(2)	1.384(3)	1.377(3)	1.377(2)	1.384(2)	1.384(2)	1.384(4)
C(5)–C(6)	1.390(2)	1.387(3)	1.388(3)	1.382(3)	1.388(2)	1.395(2)	1.389(4)
C(6)–C(1)	1.446(2)	1.454(3)	1.439(3)	1.438(2)	1.448(2)	1.447(2)	1.429(4)
C(4)–N(1)	1.456(2)	1.461(3)	1.460(2)		1.458(2)	1.460(2)	1.453(4)
C(4)–N(5)				1.462(3)			

[a] For specification of τ_1–τ_6 see Scheme 4.

This twisted conformation may obstruct effective resonance between the π-electron systems of the two connected rings. Relating to the stereoisomerism as discussed below, the naphthyl moieties of **5** are in an *anti* conformation with

Table 3 Relevant hydrogen bond parameters in the crystal structures of the compounds studied

Atoms involved		Distance		Angle
D-H···A	Symmetry	D···A	H···A	D-H···A
1a				
O(1G)–H(1G)···O(1)	x, y, z	2.732(2)	1.90	173
C(17)–H(17)···O(1)	1.5 − x, 0.5 + y, 0.5 − z	3.249(2)	2.33	163
C(13)–H(13)···O(1G)	0.5 + x, 0.5 − y, −0.5 + z	3.456(2)	2.57	155
C(41)–H(41)···O(1G)	0.5 + x, 0.5 − y, −0.5 + z	3.475(2)	2.64	146
C(35)–H(35)···C(24)[a]	1.5 − x, 0.5 + y, 0.5 − z	3.355(2)	2.60	137
1b				
O(1G)–H(1G)···O(1)	x, y, z	2.752(3)	1.91	177
C(17)–H(17)···O(1)	1.5 − x, 0.5 + y, 0.5 − z	3.208(3)	2.38	145
2a				
O(1H)–H(1H)···O(1)	x, y, z	2.600(2)	1.79	167
O(1G)–H(1G)···O(1H)	x, y, z	2.748(2)	1.93	178
C(8)–H(8)···O(1)	1 − x, −0.5 + y, 0.5 − z	3.477(3)	2.56	162
C(24A)–H(24E)···centroid(ring VII)[b]	x, y, z	3.265(3)	2.78	111
3a				
C(7)–H(7)···O(1)	−z, 1 − x, 1 − y	3.427(4)	2.62	145
C(10)–H(10)···O(1)	−z, 1 − x, 1 − y	3.388(4)	2.48	166
O(1P)···O(1P)	0.5 − x, 0.5 + z, 0.5 − y	2.252(4)		
3b				
O(1G)–H(1G)···O(1)	x, y, z	2.701(4)	1.89	161
C(13)–H(13)···O(1)	−x, 0.5 + y, 0.5 − z	3.263(2)	2.38	154
C(37)–H(37)···O(1G)	x, 0.5 − y, 0.5 + z	3.371(3)	2.52	150
C(13)–H(13)···O(1G)	−x, 0.5 + y, 0.5 − z	3.397(4)	2.69	132
4a				
O(1H)–H(1H)···O(1)	x, y, z	2.653(6)	1.82	171
C(13)–H(13)···O(1)	1.5 − x, −0.5 + y, 1.5 − z	3.382(2)	2.43	176
C(8)–H(8)···O(1)	1.5 − x, −0.5 + y, 1.5 − z	3.249(2)	2.40	148
O(1G)–H(1G)···O(1H)	x, y, z	2.736(5)	1.92	165
O(1G)–H(1G)···O(1HA)	x, y, z	2.894(5)	2.08	163
C(5)–H(5)···O(1G)	1.5 − x, −0.5 + y, 1.5 − z	3.511(2)	2.69	145
5a				
O(1G)–H(1G)···O(1)	x, y, z	2.615(4)	1.78	175
O(1F)–H(1F)···O(1)	x, y, z	2.733(4)	1.90	173
O(1H)–H(1H)···O(1G)	x, y, z	2.728(4)	2.10	132
C(43)–H(43)···O(1F)	1 − x, −0.5 + y, 1.5 − z	3.273(4)	2.54	134
C(13)–H(13)···O(1F)	x, 0.5 − y, −0.5 + z	3.389(4)	2.45	171
C(3)–H(3)···C(21)[a]	x, 0.5 − y, −0.5 + z	3.642(5)	2.74	160
C(33)–H(33)···C(20)[a]	2 − x, 0.5 + y, 1.5 − z	3.657(5)	2.78	154
C(40)–H(40)···C(15)[a]	x, 0.5 − y, 0.5 + z	3.559(5)	2.61	176
C(49)–H(49)···C(19)[a]	x, 0.5 − y, −0.5 + z	3.513(5)	2.78	135

[a] In order to gain reasonable H-bond geometries, ring carbon atoms instead of ring centroids were chosen as acceptor positions. [b] Means the centre of the corresponding ring.

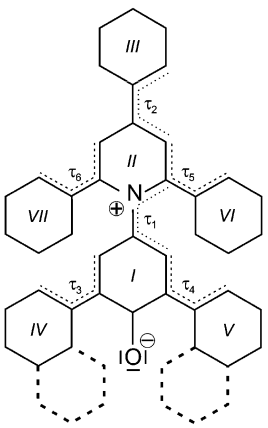

Scheme 3 Specification of torsion angles and numbering of ring components of the betaine molecules **1–5**.

reference to each other, just as the tolyl groups in the structures of the betaines **2** and **3**.

Crystallization of **1** from ethanol yielded a solvated complex **1a** [**1**·EtOH (1 : 1)] as dark blue crystals. The asymmetric part of the unit cell contains one dye molecule and one molecule of ethanol (Fig. 1). As expected, the two components of the solvated complex **1a** are linked by a short O–H···O$^-$ hydrogen bond [*d*(H(1G)···O(1) 1.90 Å].[33] The main fragment of the molecule, given by the aromatic rings *I–III*, deviates 6.8° from a linear arrangement, possibly due to packing effects. From the packing structure of **1a**, which is depicted in Fig. 2, it is apparent that the hydrogen bonded complexes are stacked along the crystallographic *a*-axis. Each stack is constructed of dimers of antiparallel arranged dye molecules with a significant overlap of their aromatic rings *II* and *III*. The shortest distance between adjacent aryl rings is 3.23 Å, suggesting π···π interaction.[34] A close packing structure is realized by nesting of molecules of neighbouring stacks which allows intermolecular C–H···π arene contacts [C(35)–H(35)···C(24) 2.60 Å, 137°].[35] The ethanol molecules are accommodated in lattice voids, each created by phenyl groups of six dye

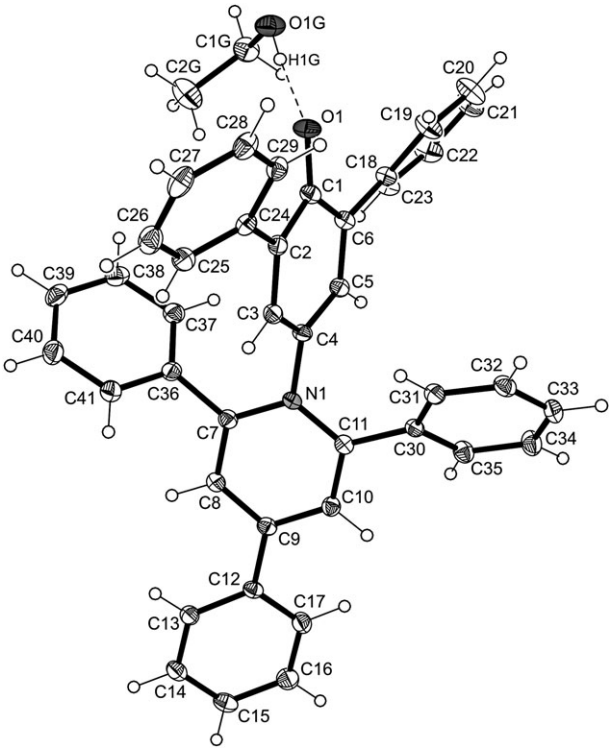

Fig. 1 Perspective view of the stoichiometric unit of solvent complex **1a** with the atom numbering scheme. The thermal displacement ellipsoids of the non-hydrogen atoms are drawn at the 40% probability level. The broken line represents a hydrogen bond.

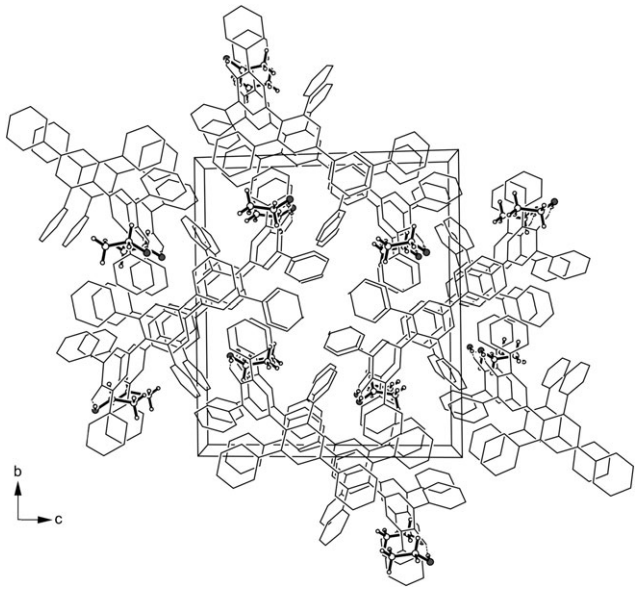

Fig. 2 Packing diagram of **1a** viewed down the crystallographic *a*-axis. The dye molecules are displayed in stick style, solvent molecules in ball-and-stick style. All hydrogen atoms of the betaine molecule are omitted for clarity. Broken lines indicate H bond interactions.

molecules. Hence, the compound **1a** can be described as a co-ordination-type clathrate[36] with pocket style topology.

A structural situation similar to **1a** is found in the complex **1b** [**1**·*i*-PrOH (1 : 1)], which is obvious from crystallographic parameters and conformational features of the dye molecule **1a** and **1b** (see Table 1 and 2). Although the molecular assemblies of both structures appear identical, the enhanced steric demand of the alcoholic guest induces a larger molecular distance along the stacking axis, as well as a disruption of C–H···π arene contacts between molecules of neighbouring stacks. Besides face-to-face arene contacts (centroid-to-centroid: 3.67 Å), there are only weak dispersive interactions between the dye molecules that stabilize the crystal structure.

Crystallization of the betaine dye **2** from methanol gives the solvated complex **2a** with the betaine : solvent stoichiometric ratio of 1 : 2. The stoichiometric unit of the complex is presented in Fig. 3. The close distance of one of two disordered positions of the methyl group (site occupancy factors, SOF: 0.81, 0.19) attached to ring *VII* indicates an intramolecular C–H(methyl)···π interaction [*d*(C(24A)···*centroid*(ring *VII*) 3.265 Å].[37] One of the methanol molecules is associated through a conventional O–H···O hydrogen bond to the phenolate oxygen of the host [O(1H)–H(1H)···O(1) 1.79 Å, 167°], whereas the hydroxy hydrogen of the second alcohol molecule is involved in guest–guest interaction [O(1G)–H(1G)···O(1H) 1.93 Å, 178°]. Moreover, the acceptor site O(1G) of this guest is associated with the arene hydrogen H(3) of a neighbouring dye molecule, so that the crystal

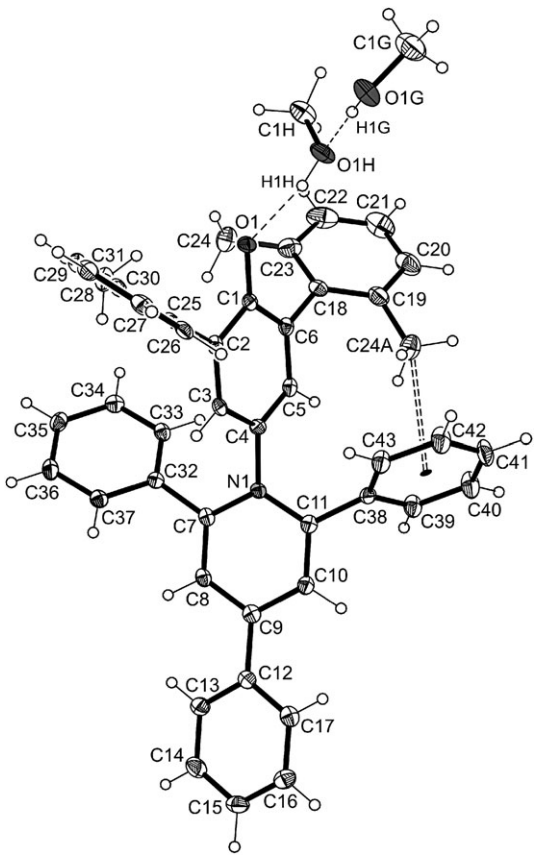

Fig. 3 Perspective view of the stoichiometric unit of solvent complex **2a** with the atom numbering scheme. The thermal displacement ellipsoids of the non-hydrogen atoms are drawn at the 40% probability level. The single broken lines represent conventional O–H···O hydrogen bonds, the double broken line indicates a weak C–H···O contact.

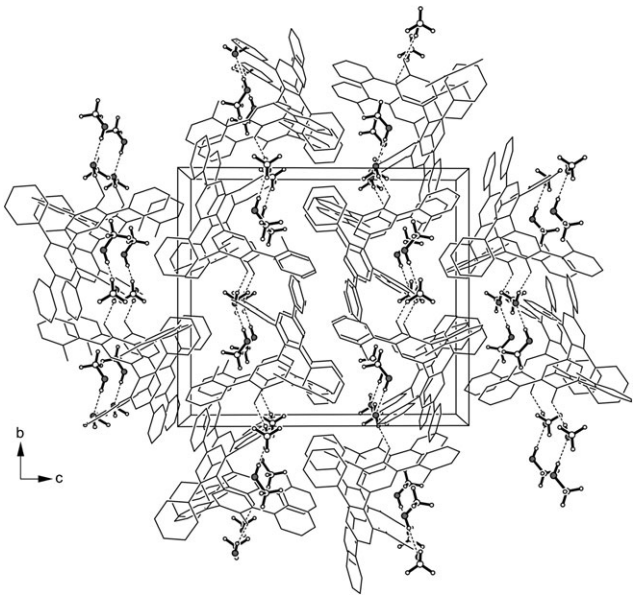

Fig. 4 Packing diagram of **2a** viewed down the crystallographic *a*-axis. The dye molecules are displayed in stick style, solvent molecules in ball-and-stick style. All hydrogen atoms of the betaine molecule are omitted for clarity. Broken lines indicate H-bond interactions.

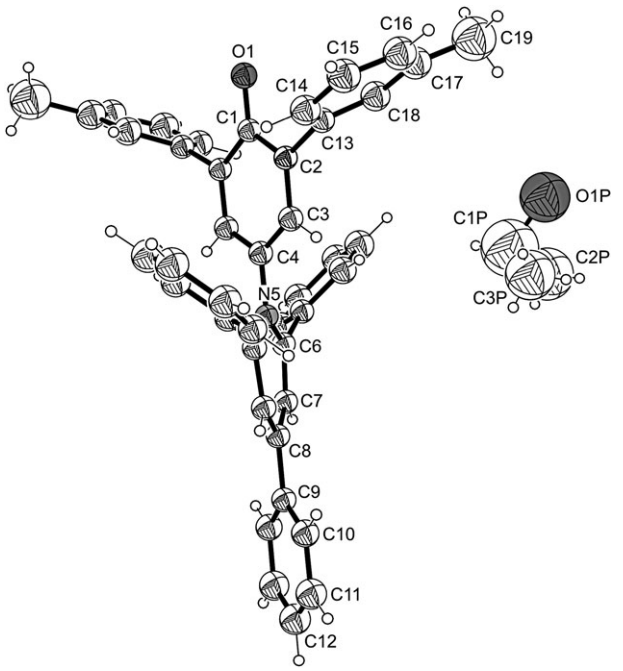

Fig. 5 Perspective view of the stoichiometric unit of solvent complex **3a**. The unique non-hydrogen positions are labelled. Only one of the disordered positions of the alcohol molecule is displayed for clarity. The thermal displacement ellipsoids of the non-hydrogen atoms are drawn at the 40% probability level.

structure of **2a** is composed of infinite chain-like dye–solvent aggregates running along the crystallographic *b*-axis (Fig. 4). This type of interaction and a variety of weaker edge-to-face arene contacts[34] exist between the dye molecules of neighbouring strands.

On crystallization of the betaine dye **3** from isopropanol, blue prisms were obtained which turned out to be a solvated complex **3a** [**3**·*i*PrOH (1 : 1)]. Because of the crystallographically imposed two-fold symmetry, the asymmetric unit cell contains one half of the dye molecule and one half of the isopropanol (Fig. 5). All phenyl rings and the phenolate ring of the dye molecule are planar within the experimental errors, while the pyridinium ring is slightly twisted around its N(5)···C(8) axis. Interestingly enough, there is no H-bond connection between the dye molecule and the alcohol. Instead, each phenolate oxygen O(1) is connected to two symmetry-related dye molecules *via* a bifurcated C–H···O contact[38] (Table 3). The packing arrangement of **3a** (Fig. 6) seems to be further stabilized by a complicated pattern of edge-to-face and stacking interactions[34,39] between the peripheral aromatic rings. On the other hand, although we were not able to localize the hydroxy hydrogen of the *i*-PrOH molecule, the O···O distance of 2.25 Å between adjacent alcoholic oxygens suggests hydrogen bond interactions between them, creating trimeric alcohol associates (Fig. 6) which are located in channel-like cavities extending along the three-fold symmetry axis of the crystal. It should be noted that the high mobility of the alcohol molecules can also be observed at low temperatures (93 K). Obviously, the tight interlocking of dye molecules creates a rigid host lattice structure with channels that show characteristic widenings with a maximum diameter of approximately 10.6 Å around the trimeric alcohol entities and empty spaces along the channel axis. Accordingly, the structure of **3a** is more likely to be termed a ''true clathrate''[40] with a channel-like topology.

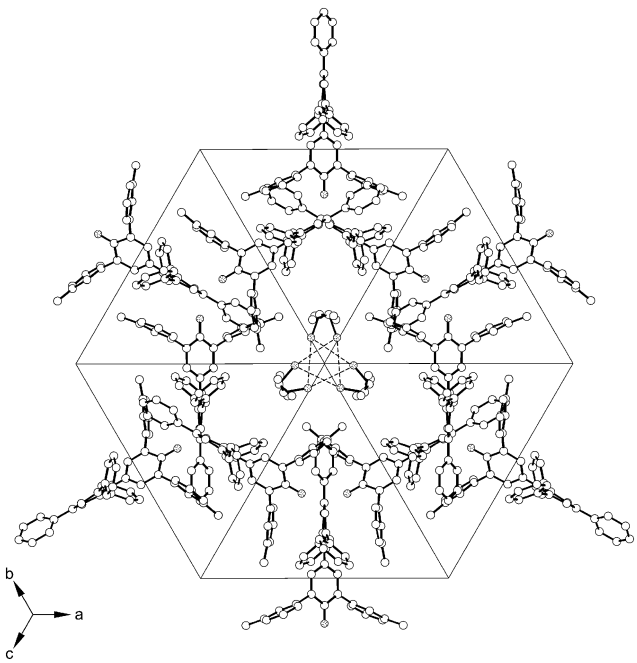

Fig. 6 Packing diagram of **3a**. All hydrogen atoms are omitted for clarity. Broken lines indicate short O···O distances, suggesting H-bond interactions.

Unlike **3a**, crystallization of **3** from *n*-BuOH yields the solvated 1 : 1 complex **3b**, in which the disordered solvent molecule (SOF 0.79, 0.21) is associated in the familiar way to the phenolate oxygen of the dye molecule. The mode of non-covalent interactions in the crystal structure of **3b**, which

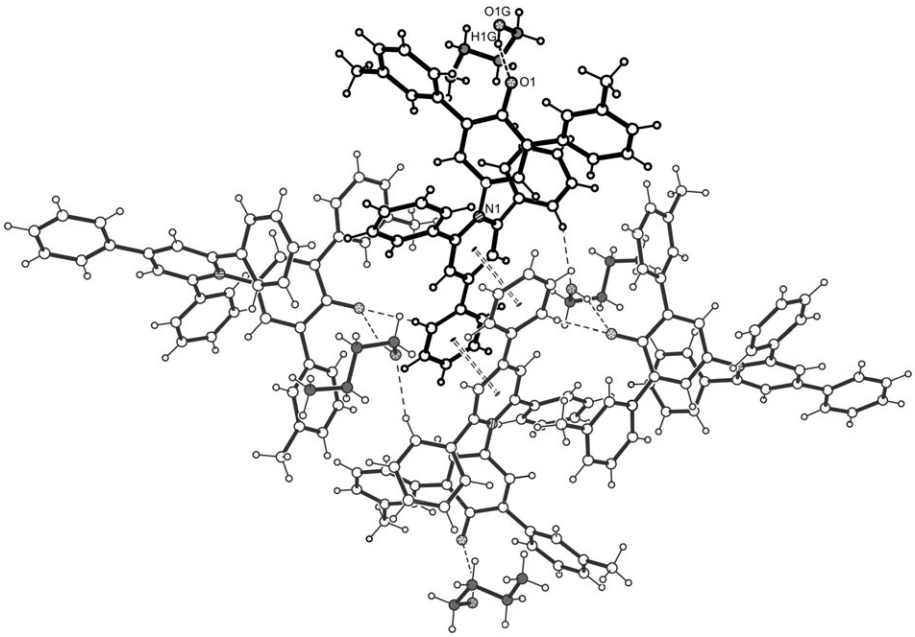

Fig. 7 Structure motif of the solvent complex **3b**. Only one of the disordered positions of the alcohol molecule is displayed for clarity. Molecules drawn in bold style represent the content of the asymmetric cell unit. Broken single lines indicate hydrogen bonds; face-to-face arene interactions are marked by broken double lines.

is illustrated in Fig. 7, comprises C–H···O hydrogen bonds [*d*(H···O) 2.51, 2.69 Å] and face-to-face interactions between aromatic rings *II* and *III* of symmetry related host molecules.

The betaine dye molecule **4** represents the *para*-methylated analogue of **1**, but yields a 1 : 2 solvent complex when crystallized from ethanol. The asymmetric part of the unit cell contains one betaine dye molecule and two molecules of the solvent, one of the latter ones disordered on two sites (SOF: 0.74 and 0.26). Consequently, a comparative consideration of the crystal structures **1a** and **4a** reveals different patterns of non-covalent interactions. In **4a**, one of the alcohol molecules is associated *via* O–H···O hydrogen bonding with a dye molecule [O(1H)–H(1H)···O(1) 1.82 Å, 171°], while its oxygen O(1H) is linked to the second solvent molecule [O(1G)–H(1G)···O(1H) 1.92 Å, 165°] (Fig. 8). Furthermore, the phenolate oxygen O(1) is involved in relatively short C–H···O hydrogen bonds to an adjacent dye molecule [*d*(H···O) 2.40, 2.43 Å]. The differences regarding the crystal structures of **1a** (Fig. 2) and **4a** (Fig. 8) are also evident from the lattice structures of the dye molecules, as well as the locations of the solvent molecules.

Crystallization of the naphthyl-substituted dye molecule **5** from methanol yielded dark coloured blocks of a solvated complex **5a** [**5**·MeOH (1 : 3)]. The asymmetric part of the unit cell contains one betaine dye molecule and three molecules of the solvent (Fig. 9). The phenolate oxygen O(1) is connected with two methanol molecules *via* hydrogen bonds [O(1G)–H(1G)···O(1) 1.78 Å, 175°, O(1F)–H(1F)···O(1) 1.90 Å, 172.6°], whereas the remaining alcohol molecule is H-bonded to the oxygen of MeOH 2 [O(1H)–H(1H)···O(1G) 2.10 Å, 132°]. Moreover, the O atom of MeOH 1 is involved in two relatively short C–H···O contacts[37] including aryl hydrogens of rings *II* and *III* of the nearest betaine molecule, hence contributing to the nearly co-planar geometry of this building unit. The overall geometry of the dye molecule deviates only slightly from C_2-symmetry. The packing arrangement of **5a** (Fig. 9) is also characterized by a variety of arene···arene interactions.[34,39] Some additional intermolecular distances indicate potential weak C–H···π contacts[35] between naphthyl moieties, arranged in the crystal in a tilted edge-to-face mode with $2.61 < d(\mathrm{H}\cdots\pi) < 2.79$ Å (Table 3). Furthermore, a naphthyl moiety and the electron-deficient pyridinium ring of an adjacent dye molecule, which are nearly parallel to each other, have a centroid···centroid distance of 4.65 Å, possibly suggesting a weak π···π interaction.

Stereoisomerism of compounds 9d and 5

The ^{1}H and ^{13}C NMR spectra of compound **9d** obtained in [D_2]tetrachloroethane (TClE) at $T = 20$ °C show the presence of two isomeric forms in an approximately 50 : 50 mixture owing to restricted rotation about the naphthyl–nitrophenol bond. Hence, these two atropisomeric stereoisomers of **9d** correspond to the *meso* compound and the racemic mixture of the enantiomers (Scheme 4). Variable temperature NMR analysis revealed line shape changes in proton signals and collapse of split carbon signals determined in the temperature range between 20 and 60 °C. While the ^{13}C NMR of compound **9d** in [D_2]TClE solution at 20 °C shows a total of 24 signals, a consecutive decrease to 14 signals (expected number of signals for free bond rotation) was observed in the course of the temperature increase (see Experimental). This study allows us to estimate the coalescence temperature for free rotation of the naphthyl–nitrophenol bond as around 55 °C, corresponding to a rotational barrier of about 16.9(5) kcal mol^{-1}. A rather similar conformational behaviour based on NMR data in C_6D_6 solution, that is a barrier to naphthyl rotation of

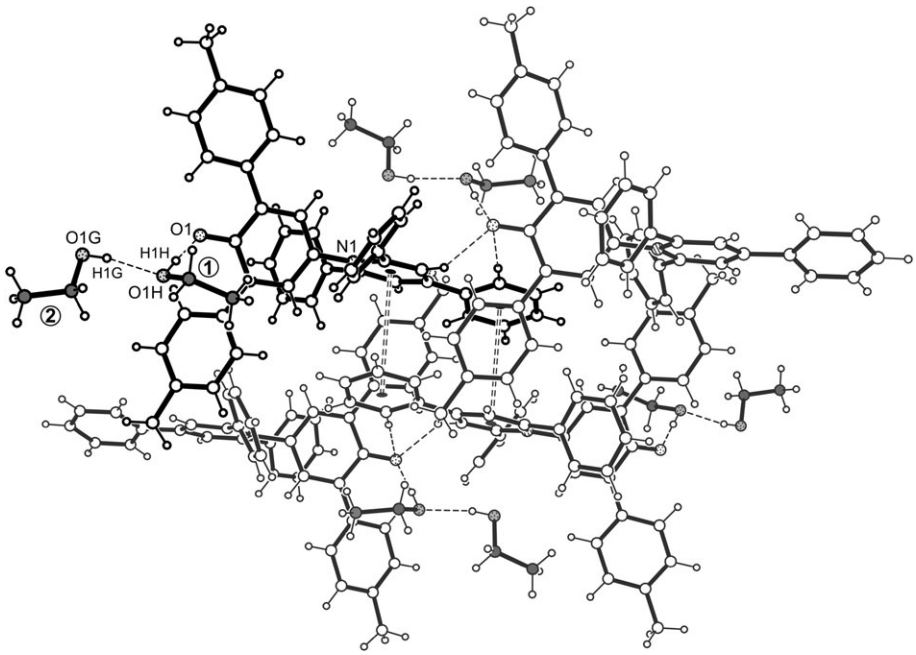

Fig. 8 Structure motif of the solvent complex **4a**. Only one of the disordered positions of the alcohol molecule 1 is displayed for clarity. Molecules drawn in bold style represent the content of the asymmetric cell unit. Broken single lines indicate hydrogen bonds; face-to-face arene interactions are marked by broken double lines.

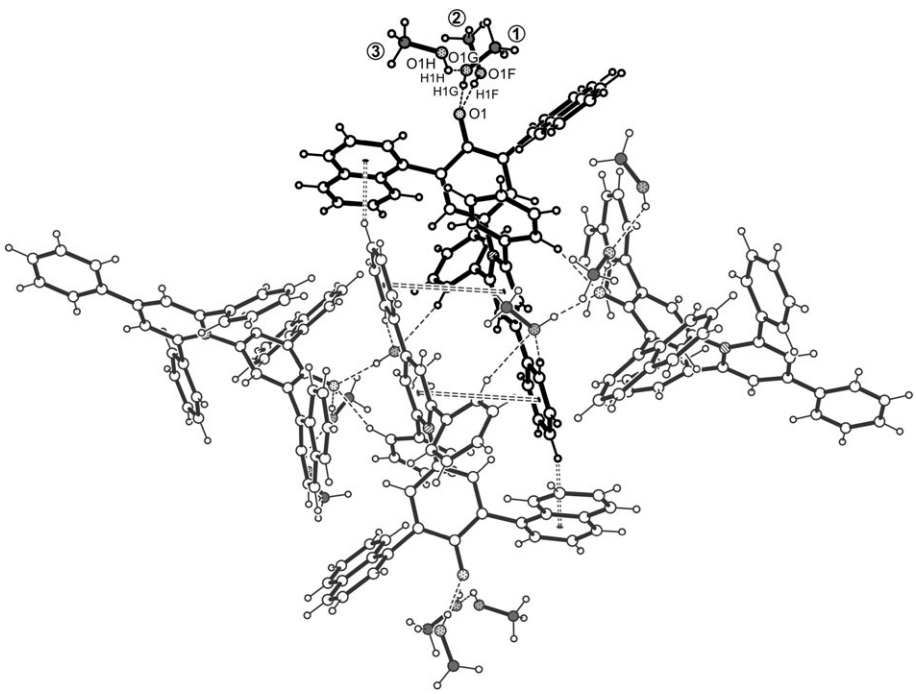

Fig. 9 Structure motif of the solvent complex **5a**. Molecules drawn in bold style represent the content of the asymmetric unit cell. Broken single lines indicate hydrogen bonds; face-to-face arene interactions are marked by broken double lines.

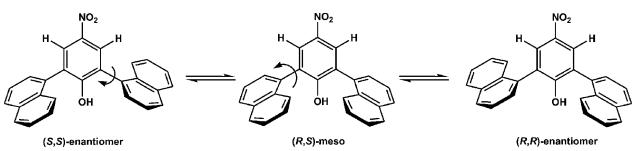

Scheme 4 Rotational isomerism of compound **9d**.

18.0 kcal mol^{-1} at 67 °C, has previously been reported for the parent compound 2,6-bis(1-naphthyl)phenol lacking the *p*-nitro group.[41]

The somewhat increased rotational barrier found for the parent phenol molecule is very likely attributable to both the different solvents used for the NMR determinations and

Table 4 Vis. absorption maxima (λ_{max}, nm) of diluted solutions (10^{-3} M) of the betaine dyes **2–5**, measured in solvents of different polarity at room temperature (25 °C) with corresponding E_T values (kcal mol^{-1})[a], including E_T(**30**) values

Solvent	**1** (E_T **30**)[b]	**2** λ_{max} (E_T)	**3** λ_{max} (E_T)	**4** λ_{max} (E_T)	**5** λ_{max} (E_T)
Methanol	(55.4)	496 (57.6)	516 (55.4)	521 (54.9)	504 (56.7)
Ethanol	(51.9)	540 (52.9)	554 (51.6)	558 (51.2)	541 (52.8)
1-Butanol	(49.7)	567 (50.4)	580 (49.3)	582 (49.1)	566 (50.5)
2-Propanol	(48.4)	584 (48.9)	600 (47.7)	602 (47.5)	585 (48.9)
Dichloromethane	(40.7)	690 (41.4)	708 (40.4)	714 (40.0)	681 (42.0)

[a] Calculated according to ref. 14. [b] Taken from ref. 5.

the additional nitro substituent in the case of **9d**. However, coming to a clear decision on the real consequences of these facts is a problem. A previous study has shown that *o*-phenylphenols remain monomeric in solution with strong evidence for π-hydrogen bonding between the OH proton and an *o*-phenyl ring.[42] Hence, measurement of the rotational barrier should be affected by the polarity and hydrogen bond acceptor ability of the solvent. On the other hand, one should expect an increase of the OH acidity caused by the nitro group of **9d** having an influence on the intramolecular π-hydrogen bonding and, thus, being connected with the rotational flexibility of the molecule.

A conformational behaviour similar to the nitrophenol **9d** was observed for the betaine **5**, featuring a corresponding structural situation for the two 1-naphthyl units of the molecule. But, due to the betaine structure of **5**, the O atom refers now to an anionic phenolate oxygen instead of the hydroxyl group of **9d**. From this angle, the rotational barrier of the naphthyl–nitrophenolate bond of **5** is expected to be somewhat lower compared to **9d**, since π-hydrogen bonding cannot produce an effect. However, owing to the neighbouring phenyl residues of the pyridinium moiety, an additional steric hindrance may become effective.[6] Putting it in concrete terms, the atropical stereoisomerism of the compound **5** is becoming apparent in a split of signals both in the ^{1}H and ^{13}C NMR spectra in [D$_2$]TClE at 20 °C with line shape changes and consecutive decrease of signals on temperature increase. At 20 °C, the ^{13}C NMR spectrum shows 45 signals that collapsed to 22 resolved signals at 80 °C (25 individual signals expected for free rotation of the molecule). The four carbon signals ranging between 157 and 158 ppm, assigned to the 1-PhO C-atom,[14,43] suggests the presence of four atropisomeric species at 20 °C, while a singlet at 157.7 ppm is observed at 80 °C, indicating rapid interconversion of the atropisomers. We can therefore estimate that the barrier to free rotation in **5** is higher than the value of 16.0 kcal mol^{-1} at 55 °C measured for the related nitrophenol **9d**. Considering a coalescence temperature for the betaine **5** around 75 °C, the corresponding rotational barrier is about 18.1(5) kcal mol^{-1}. Analysis of the crystals obtained from a solution of **5** in methanol by X-ray diffraction (see above) showed the presence of a particular chiral form as both enantiomers in the unit cell, featuring the molecule with naphthyl moieties rotated in an *anti* orientation and twisted phenyl groups.

Solvatochromic properties of the betaine dyes

The positions of the solvatochromic long wavelength intramolecular charge-transfer (CT) absorption band (λ_{max}, nm) of the new betaine dyes **2–5** in various solvents of different polarity have been determined. These data, together with the corresponding electronic transition energies E_T(**2**)–E_T(**5**) in kcal mol^{-1}, are listed in Table 4. In analogy to the prior standard betaine dye **1**,[5] included in Table 4, the new dyes **2–5** also exhibit an extraordinary negative solvatochromism. In changing the solvent from polar methanol to less polar dichloromethane, the hypsochromic shifts ($\Delta\lambda_{max}$) of the intramolecular CT absorption band range between −177 and −194 nm, dependent on the respective dye. This corresponds to an increase of their molar transition energies E_T of between 14.7 and 16.2 kcal mol^{-1}. At a rough estimate, these values are similar to those found for **1**[5] and related alkyl substituted derivatives of **1**.[14] At most, the *o*-tolyl and 1-naphthyl derivatives (**2** and **5**, respectively) behave a little different regarding the hypsochromic shifts and ΔE_T, as compared with the other betaines, which is possibly a consequence of the steric conditions owing to these particular substituents. Actually, in detail, there are other differences between the individual compounds the causes of which are difficult to explain, however. Nevertheless, it is shown that with increasing solvent polarity, the high dipolar ground state of the new betaine dyes **2–5** is increasingly stabilized by differential solvation, relative to the less dipolar CT excited state, with the observed hypsochromic band shift as consequence.

Conclusion

Following the established procedure for the preparation of *para*-pyridinium *N*-phenoxides,[4,28,29] four new betaine dyes **2–5** of the Reichardt's type have been synthesized. They feature two tolyl substituents in different attachment or two 1-naphthyl groups in the phenoxide moiety, instead of simple phenyls as for the standard betaine dye **1**. Based on the position of the long wavelength intramolecular charge-transfer absorption band in solvents of different polarity, the negative solvatochromism and, thus, the calculated E_T-values of the betaine dyes **2–5** fall between the standard compound **1**[5] and known related alkyl derivatives of **1**.[14] Therefore, both the present modes of methyl substitution and the exchange of phenyl for 1-naphthyl groups in **1** do not show unusual effects on the solvatochromatic properties.

From variable-temperature solution NMR measurement, the betaine **5**, as well as the intermediate compound **9d**, were determined to exist as rotational stereoisomers at ambient temperature and free rotating molecules at increased temperature. In the crystalline alcoholic complexes of **2–5**, as well as the

unsubstituted parent compound **1**, *i.e.* **1a**, **1b**, **2a**, **3a**, **3b**, **4a** and **5a**, the betaine molecules are considerably distorted around the arene–arene and arene–heteroarene bonds, preventing significant conjugation. Particularly, in the cases of **2**, **3** and **5**, the tolyl and naphthyl moieties are all in an *anti* conformation with reference to each other. Moreover, it is shown by the dihedral angles in the range between 55 and 75°, involving the planes of the phenoxide and pyridinium rings, that the ground state structures of the present betaines are genuine zwitterions. This is in agreement with earlier observations,[15,16] but actually conflicting with required mobility of electron density between the two rings upon excitation,[2] being previously discussed along different lines.[12,44] However, it is also not unlikely that the molecular geometries differ between crystalline and solution state, so as to make normal π-orbital interaction possible. Nevertheless, in accordance with previous computer simulation studies,[45] it is demonstrated with the crystal structures of the present solvent complexes, except **3a**, that the preferred docking site for the hydrogen donor alcohol molecules is the phenolate oxygen of the dye molecules. Generally, the molecular structures in the crystals are rather similar and not in obvious contrast to previous reports,[12,15,16] unlike the packing modes, showing more developed differences with modification of the lateral aryl groups.

In addition to the increase of insight in the structural features of this important compound class, the new betaine dyes may provide a basis for future quantum chemical calculations in order to improve the knowledge of the excitation process.[46] Other promising aspects are to use these solvatochromic dyes as sorptive transducer elements in optical chemical sensors[9,13,47] or in the development of nonlinear optical materials.[10,48]

Experimental

Methods and materials

Melting points: Kofler melting point microscope (uncorrected). ^{1}H and ^{13}C NMR (internal standard TMS): Bruker AVANCE DPX 400 and AVANCE DPX 500. MS: A.E.I. MS 50, Kratos FAB-MS Concept 1H, and Hewlett Packard GC-MS 5989 A/5890 II. Elemental analysis: Heraeus CHN rapid analyzer. TLC-analysis: aluminium sheets precoated with silica gel 60 F_{254} (Merck). Column chromatography: silica gel (63–100 μm, Merck). Organic solvents were purified by standard procedures.[49] Compound **1** was purchased from Aldrich.

Synthesis

The starting ketones **7a–7d** were synthesized from **6a–d** using two alternative literature procedures (A[31] and B[32]) as specified in Scheme 2. The data obtained for these compounds (**7a**,[50,51] **7b**,[50,52,53] **7c**,[54–56] **7d**[57,58]) correspond with the literature. The triphenylpyrylium hydrogen sulfate (**11**)[59] and 2-nitromalonaldehyde-Na[60] (**8**) were prepared as described.

General procedure.[30,50] Synthesis of nitrophenols 9a–d. To a stirred mixture of the respective ketone **7a–d** (10 mmol) in degassed ethanol (6 mL) and THF (6 mL) was added a solution of 2-nitromalonaldehyde-Na monohydrate (**8**) (12 mmol) in aqueous NaOH (1 M, 26 mL). The mixture was kept stirring under N_2 at room temperature or slightly elevated temperature for between 20 and 96 h. The solid was filtered off and most of the solvent removed under reduced pressure. Water was refilled and conc. hydrochloric acid added until complete precipitation of the crude phenol. Details including procedure of purification and data of the individual compounds are given below.

2,6-Bis(2-methylphenyl)-4-nitrophenol (9a). 1,3-Bis(2-methylphenyl)propan-2-one (**7a**) and (**8**) were reacted at 30–35 °C for 20 h. Purification by column chromatography (SiO_2, eluent: toluene) yielded 53% colourless crystals; mp 192 °C (lit.[50] 192–193 °C). IR (KBr): $\tilde{\nu}$ = 3446 cm^{-1} (s, O–H), 3060, 3012, 2920, 2860 (w, C–H), 1600, 1584 (m, Ar), 1516 (s, N–O), 1455, 1380 (m, C–H), 1325 (s, C–NO_2). ^{1}H NMR (400 MHz, [D6]DMSO): δ = 2.16 (s, 6 H, CH_3), 7.25–7.37 (m, 8 H, Ar–H), 7.91 (s, 2 H, Ar–H), 9.75 (s, 1 H, OH) ppm. ^{13}C NMR (100 MHz, [D6]DMSO): δ = 19.47 (CH_3), 125.58, 126.02, 128.27, 129.96, 130.10, 130.19, 136.37, 136.57, 139.41 (C–NO_2), 157.73 (C–OH) ppm. MS (GC): m/z = 319 [M]$^+$. $C_{20}H_{17}NO_3$ (319.36): calcd. C 75.22, H 5.36, N 4.39; found C 75.51, H 5.51, N 4.23%.

2,6-Bis(3-methylphenyl)-4-nitrophenol (9b). 1,3-Bis(3-methylphenyl)propan-2-one (**7b**) and (**8**) were reacted at room temperature for 96 h. The solid which was present immediately after completion of the reaction was collected and recrystallized from ethanol to yield a first crop of the product. A second crop was isolated *via* treatment of the filtrate as specified in the general procedure, followed by column chromatography (SiO_2, eluent: toluene) to give a total yield of 72% colourless crystals; mp 146 °C (lit.[50] 145 °C). IR (KBr): $\tilde{\nu}$ = 3478 cm^{-1} (s, O–H), 3094, 3060, 3037, 2949, 2917, 2857 (w, C–H), 1609, 1581 (m, Ar), 1524 (s, N–O), 1483, 1375 (m, C–H), 1334 (s, C–NO_2). ^{1}H NMR (400 MHz, [D6]DMSO): δ = 2.37 (s, 6 H, CH_3), 7.23–7.40 (m, 8 H, Ar–H), 8.19 (s, 2 H, Ar–H), 9.89 (s, 1 H, OH) ppm. ^{13}C NMR (100 MHz, [D6]DMSO): δ = 21.12 (CH_3), 124.98, 126.51, 128.50, 128.63, 129.96, 131.14, 136.56, 137.74 (Ar), 140.15 (C–NO_2), 157.36 (C–OH) ppm. MS (GC): m/z = 319 [M]$^+$. $C_{20}H_{17}NO_3$ (319.36): calcd. C 75.22, H 5.36, N 4.39; found C 75.09, H 5.12, N 4.17%.

2,6-Bis(4-methylphenyl)-4-nitrophenol (9c). 1,3-Bis(4-methylphenyl)propan-2-one (**7c**) and **8** were reacted at room temperature for 96 h. Purification by column chromatography (SiO_2, eluent: toluene) yielded 80% colourless crystals; mp 136 °C (lit.[50] 137 °C). IR (KBr): $\tilde{\nu}$ = 3487 cm^{-1} (s, O–H), 3034, 2920, 2860, (w, C–H), 1613, 1584 (m, Ar), 1505 (s, N–O), 1448, 1385 (m, C–H), 1328 (s, C–NO_2). ^{1}H NMR (400 MHz, [D6]DMSO): δ = 2.36 (s, 6 H, CH_3), 7.29 (d, ^3J = 8 Hz, 4 H, Ar–H), 7.47 (d, ^3J = 8 Hz, 4 H, Ar–H), 7.98 (s, 2 H, Ar–H), 9.83 (s, 1 H, OH) ppm. ^{13}C NMR (100 MHz, [D6]DMSO): δ = 20.86 (CH_3), 124.75, 129.61, 129.26, 130.96, 133.73, 137.30 (Ar), 140.13 (C–NO_2), 157.49 (C–OH) ppm. MS (GC): m/z = 319 [M]$^+$. $C_{20}H_{17}NO_3$ (319.36): calcd. C 75.22, H 5.36, N 4.39; found C 74.90, H 5.37, N 4.34%.

2,6-Di(1-naphthyl)-4-nitrophenol (9d). 1,3-Di(1-naphthyl)-propan-2-one (**7d**) and **8** were reacted at room temperature for 48 h. Purification by column chromatography (SiO_2,

eluent: toluene) yielded 61% light yellow crystals; mp 196 °C. IR (KBr): $\tilde{\nu}$ = 3493 cm^{-1} (s, O–H), 3053, 2927, 2851 (w, C–H), 1619, 1584 (m, Ar), 1524 (s, N–O), 1448, 1388 (m, C–H) 1328 (s, C–NO_2). ^{1}H NMR (400 MHz, [D2]TClE, 20 °C): δ = 5.73 (s, 1 H, OH), 7.43–7.66 (m, 10 H, Ar–H), 7.88–7.95 (m, 4 H, Ar–H), 8.27 (s, 2 H, Ar–H) ppm. ^{1}H NMR (400 [D2]TClE, 60 °C): δ = 5.64 (s, 1 H, OH), 7.40–7.80 (m, 1 OH, Ar–H), 7.80–8.00 (m, 4 H, Ar–H), 8.30 (s, 2 H, Ar–H). ^{13}C NMR (100 MHz, [D2]TClE, 20 °C): δ = 125.3, 125.4, 126.00, 126.04, 126.9, 127.34, 127.36, 127.4, 128.1, 128.2, 128.6, 128.7, 129.0, 129.1, 129.9, 131.5, 131.6, 132.6, 132.7, 134.0 (Ar), 141.3, 141.4 (C–NO_2) 156.8, 156.9 (C–OH) ppm. ^{13}C NMR (100 MHz, [D2]TClE, 60 °C): δ = 125.3, 126.0, 126.8, 127.3, 127.4, 128.3, 128.6, 129.0, 129.9, 131.8, 132.8, 134.2 (Ar), 141.6 (C–NO_2), 156.8 (C–OH) ppm. MS (GC): m/z = 391 $[M]^+$. $C_{26}H_{17}NO_3$ (391.42): calcd. C 79.78, H 4.38, N 3.58; found C 79.32, H 4.31, N 3.40%.

General procedure.[61] Synthesis of aminophenols 10a–d. A suspension of the corresponding nitrophenol **9a–d** (2.5 mmol) and of 10% Pd/C (50 mg) in dry ethanol (25 mL) was hydrogenated in a Parr apparatus at 2 atm and at room temperature for 5 h. The catalyst was filtered off under argon and the product solution containing **10a–d**, respectively, was directly used in order to avoid oxidation decomposition of the compounds. Evaporation of a sample showed complete reaction (TLC analysis).

General procedure.[29] Synthesis of the betaine dyes 2–5. To the above solutions of the corresponding aminophenol **10a–d** (2.5 mmol) in EtOH were added under Ar 2,4,6-triphenylpyrylium hydrogensulfate (**11**) (1.0 g, 2.5 mmol) and anhydrous sodium acetate (1.0 g, 12 mmol). The mixture was heated to reflux for 3 h. Then, 5% aqueous NaOH solution (7.5 mL) was added to the hot solution. The major part of EtOH is removed under reduced pressure, refilled with water, condensed again and so on until complete precipitation of the betaine. The precipitate was collected, washed with water and purified by column chromatography (SiO_2, eluent: EtOH). Details and data of the individual compounds are given below.

2,6-Bis(2-methylphenyl)-4-(2,4,6-triphenyl-1-pyridinio)phenolate (2). From aminophenol **10a** and **11** in 35% yield as a blue solid; mp 218 °C. IR (KBr): $\tilde{\nu}$ = 3053, 3015, 2952 cm^{-1} (w, C–H), 1619, 1597 (s, Ar), 1473, 1359 (s, C–H). ^{1}H NMR (400 MHz, $CDCl_3$): δ = 2.05 (s, 6 H, CH_3), 6.37 (s, 3 H, Ar–H), 6.72 (d, ^3J = 6.9 Hz, 2 H, Ar–H), 6.90–7.10 (m, 5 H, Ar–H), 7.26 (s, 3 H, Ar–H), 7.30–7.50 (m, 8 H, Ar–H), 7.55–7.65 (m, 3 H, Ar–H), 7.85 (d, ^3J = 6.8 Hz, 1 H, Ar–H), 8.06 (s, 2 H, Py-H) ppm. ^{13}C NMR (100 MHz, $CDCl_3$): δ = 20.32 (CH_3), 124.18, 125.97, 126.62, 127.36, 128.02, 129.51, 130.09, 130.27, 131.01, 131.25, 131.71, 132.00, 133.21, 133.72, 135.53, 135.66, 138.52, 142.09, 157.20 (Ar, 3,4,5-Py, 2,3,4,5,6-PhO), 158.96, (2,6-Py) 165.22 (1-PhO) ppm. MS (HR): m/z = 579.2543 $[M]^+$. $C_{43}H_{33}NO{\cdot}H_2O$ (597.27): calcd. C 86.40, H 5.90, N 2.34; found: C 85.93, H 5.94, N 2.14%.

2,6-Bis(3-methylphenyl)-4-(2,4,6-triphenyl-1-pyridinio)phenolate (3). From aminophenol **10b** and **11** in 54% yield as a blue solid; mp 121–124 °C. IR (KBr): $\tilde{\nu}$ = 3056, 3028, 2917, 2863 cm^{-1} (w, C–H), 1616, 1597 (s, Ar), 1461, 1356 (s, C–H). ^{1}H NMR (400 MHz, $CDCl_3$): δ = 2.28 (s, 6 H, CH_3), 6.40 (s, 2 H, Ar–H), 6.90 (d, ^3J = 7.4 Hz, 2 H, Ar–H), 6.95–7.10 (m, 6 H, Ar–H), 7.25–7.40 (m, 10 H, Ar–H), 7.55–7.65 (m, 3 H, Ar–H), 7.80–7.90 (m, 2 H, Ar–H), 8.05 (s, 2 H, Py-H) ppm. ^{13}C NMR (100 MHz, $CDCl_3$): δ = 21.39 (CH_3), 117.93, 125.30, 125.51, 125.83, 126.34, 127.60, 127.68, 128.74, 129.10, 129.59, 129.81, 130.11, 132.05, 133.68, 134.02, 135.98, 140.37, 153.50 (Ar, 3,4,5-Py), 156.36 (2,6-Py), 169.10 (1-PhO) ppm. MS (FAB): m/z = 580.2. $[M]^+$. $C_{43}H_{33}NO{\cdot}2H_2O$ (615.28): calcd. C 83.87, H 6.06, N 2.27; found: C 83.39, H 5.84, N 2.26%.

2,6-Bis(4-methylphenyl)-4-(2,4,6-triphenyl-1-pyridinio)phenolate (4). From aminophenol **10c** and **11** in 43% yield as a blue solid; mp 200 °C. IR (KBr): $\tilde{\nu}$ = 3056, 3025, 2917, 2860 cm^{-1} (w, C–H), 1622, 1597 (s, Ar), 1492, 1397, 1356 (s, C–H). ^{1}H NMR (400 MHz, $CDCl_3$): δ = 2.28 (s, 6 H, CH_3), 6.51 (s, 2 H, Ar–H), 7.00 (d, ^3J = 7.4 Hz, 2 H, Ar–H), 7.20–7.30 (m, 7 H, Ar–H), 7.35–7.50 (m, 8 H, Ar–H), 7.60–7.65 (m, 4 H, Ar–H), 7.80–7.90 (m, 2 H, Ar–H), 8.04 (s, 2 H, Py-H) ppm. ^{13}C NMR (100 MHz, [D6]DMSO): δ = 20.77 (CH_3), 125.04, 128.16, 128.66, 128.72, 128.78, 128.89, 129.25, 129.53, 129.87, 130.10, 132.45, 133.53, 133.69, 134.76, 136.27, 144.53, 154.86 (Ar, 3,4,5-Py), 156.66 (2,6-Py), 164.83 (1-PhO) ppm. MS (HR): m/z = 579.2538 $[M]^+$. $C_{43}H_{33}NO{\cdot}2H_2O$ (615.28): calcd. C 83.87, H 6.06, N 2.27; found: C 83.14, H 6.02, N 2.16%.

2,6-Di(1-naphthyl)-4-(2,4,6-triphenyl-1-pyridinio)phenolate (5). From aminophenol **10d** and **11** in 56% yield as a blue solid; mp > 300 °C. IR (KBr): $\tilde{\nu}$ = 3050, 3003 cm^{-1} (w, Ar), 1619, 1594 (s, Ar). ^{1}H NMR (500 MHz, [D2]TClE, 20 °C): δ = 6.63, 6.65, 6.83, 6.85, 7.00, 7.03, 7.12, 7.14 (6 H, Ar–H), 7.27–7.69 (m, 16 H, Ar–H), 7.82–7.90 (m, 6 H, Ar–H), 8.18 (s, 2 H, Py-H) ppm. ^{1}H NMR (500 MHz, [D2]TClE, 80 °C): δ = 6.82 (s, 2 H, Ar–H), 6.96 (s, 2 H, Ar–H), 7.06, 7.13–7.39 (d, 2 H, Ar–H), 7.32–7.66 (m, 16 H, Ar–H), 7.83–7.95 (m, 6 H, Ar–H), 8.19 (s, 2 H, Py-H) ppm. ^{13}C NMR (125 MHz, [D2]TClE, 20 °C): δ = 123.8–134.0 (39 signals, Ar, 3,4,5-Py, 2,3,4,5,6-PhO) 152.46, 152.52 (2,6-Py), 157.3, 157.5, 157.7, 158.0 (1-PhO) ppm. ^{13}C NMR (125 MHz, [D2]TClE, 80 °C): δ = 125.0, 125,7, 126.2, 126.6, 127.0, 127.9, 128.4, 128.7, 128.9, 129.6, 130.2, 130.5, 130.8, 131.2, 131.8, 132.5, 132.8, 133.5, 134.2, 134.3 (Ar, 3,4,5-Py, 2,3,4,5,6-PhO), 152.3 (2,6-Py), 157.7 (1-PhO) ppm. MS (HR): m/z = 651.2560 $[M]^+$. $C_{49}H_{33}NO{\cdot}H_2O$ (669.27): calcd. C 87.86, H 5.27, N 2.09; found: C 87.93, H 5.40, N 1.94%.

Crystallography

Crystals of the complexes suitable for single crystal X-ray diffraction studies were obtained by slow solvent evaporation of solutions of the respective betaine dyes in the corresponding solvent. Information concerning the crystallographic data and the structure refinement calculations of the three compounds is summarized in Table 1. Data collection of **1a**, **1b**, **2a**, **3b**, **4a** and **5a** was carried out on a Kappa APEX II diffractometer (Bruker AXS), using ω- and ϕ-scans. The collected data were corrected for Lorentz and polarisation effects. The structures

were solved by direct methods[62] and refined by full-matrix least squares calculations on F^2.[63] The non-hydrogen positions and disorder sites were refined together with their anisotropic displacement parameters, and the H atoms and H disorder sites were treated isotropically. All H positions were held riding on the respective parent O or C atoms during the subsequent calculations. Data of **3a** were collected on a Enraf-Nonius CAD-4 diffractometer. Crystals of **3a** turned out to show weak scattering power which allowed data collection up to a Θ-value of 65°. The cell parameters were determined and refined using the CAD4-Express program.[64] Two standard reflections, monitored every 120 min, showed a crystal decay of 13% during the entire data collection procedure. Reflection data were corrected for Lorentz and polarization effects using the XCAD4 program.[65] The structures were solved by application of direct methods,[62] and refined by full-matrix least-squares calculations on F^2 with anisotropic vibration displacement parameters for all non-hydrogen atom positions.[63] All carbon-bonded H atoms were given positions calculated using geometric evidence, whereas the hydroxyl hydrogen could not be located from a difference electron density map.

Acknowledgements

Financial support by the Deutsche Forschungsgemeinschaft (DFG) and the Fonds der Chemischen Industrie is gratefully acknowledged. EW thanks Prof. C. Reichardt and Dr U. Böhme for helpful discussion.

References

1 C. Reichardt, *Solvent and Solvent Effects in Organic Chemistry*, Wiley-VCH, Weinheim, 2003.
2 C. Reichardt, *Chem. Soc. Rev.*, 1992, **21**, 147.
3 C. Reichardt, S. Asharin-Fard, A. Blum, M. Eschner, A.-M. Mehranpour, P. Milart, T. Niem, G. Schäfer and M. Wilk, *Pure Appl. Chem.*, 1993, **65**, 2593.
4 K. Dimroth, C. Reichardt, C. Siepmann and T. Bohlmann, *Justus Liebigs Ann. Chem.*, 1963, **661**, 1.
5 C. Reichardt, *Chem. Rev.*, 1994, **94**, 2319.
6 P. Plieninger and H. Baumgärtel, *Liebigs Ann. Chem.*, 1983, **1983**, 860.
7 H. Langhals, *Fresenius' Z. Anal. Chem.*, 1981, **308**, 441.
8 H. Langhals, *Anal. Lett.*, 1991, **23**, 2243.
9 F. L. Dickert and A. Haunschild, *Adv. Mater.*, 1993, **5**, 887.
10 M. S. Paley and M. Harris, *J. Org. Chem.*, 1991, **56**, 568.
11 A. J. M. van Beijnen, R. J. M. Nolte and W. Drenth, *Recl. Trav. Chim. Pays-Bas*, 1986, **105**, 255.
12 M. S. Paley, E. J. Meehan, C. D. Smith, F. E. Rosenberger, S. C. Howard and J. M. Harris, *J. Org. Chem.*, 1989, **54**, 3432.
13 D. Crowther and X. Liu, *J. Chem. Soc., Chem. Commun.*, 1995, 2445.
14 C. Reichardt, S. Löbbecke, A.-M. Mehranpour and G. Schäfer, *Can. J. Chem.*, 1998, **76**, 686.
15 R. Allmann, *Z. Kristallogr.*, 1969, **128**, 115.
16 K. Stadnicka, P. Milart, A. Olech and P. K. Olszewski, *J. Mol. Struct.*, 2002, **604**, 9.
17 S. M. Aldoshin, Y. R. Tymyanskii, O. A. Dyachenko, L. O. Atovmyan, M. I. Knyazhanskii and G. N. Dorofeenko, *Izv. Akad. Nauk SSSR, Ser. Klum (Russ. Chem. Bull.)*, 1981, 2270.
18 P. Milart, D. Mucha and K. Stadnicka, *Liebigs Ann.*, 1995, 2049.
19 P. Milart and K. Stadnicka, *Eur. J. Org. Chem.*, 2001, 2337.
20 J. Baran, A. J. Barnes, M. Drozd, J. Janczak and M. Sledz, *J. Mol. Struct.*, 2001, **598**, 117.
21 Z. Dega-Szafran, A. Katrusiak and M. Szafran, *J. Mol. Struct.*, 2009, **936**, 9.
22 Z. Dega-Szafran, Z. Fojud, A. Katrusiak and M. Szafran, *J. Mol. Struct.*, 2009, **928**, 99.
23 M. Szafran, P. Barczyuski, A. Komasa and Z. Dega-Szafran, *J. Mol. Struct.*, 2008, **887**, 20.
24 Z. Dega-Szafran, A. Katrusiak and M. Szafran, *J. Mol. Struct.*, 2008, **875**, 577.
25 J. W. Steed and J. Atwood, *Supramolecular Chemistry*, Wiley, Chichester, 2000.
26 E. Weber, in *Kirk Othmer Encyclopedia of Chemical Technology*, ed. J. I. Kroschwitz, Wiley, New York, 4th edn, Suppl., 1998, p. 352.
27 G. R. Desiraju, *Angew. Chem.*, 1995, **107**, 2541 (*Angew. Chem., Int. Ed. Engl.*, 1995, **34**, 2311).
28 B. P. Johnson, B. Gabrielsen, M. Matulenko, J. G. Dorsey and C. Reichardt, *Anal. Lett.*, 1986, **19**, 939.
29 M. A. Kessler and O. S. Wolfbeis, *Synthesis*, 1988, 635.
30 H. B. Hill, C. A. Soch and G. Oenslager, *Am. Chem. J.*, 1900, **24**, 1.
31 E. Schmidt, *Ber. Dtsch. Chem. Ges.*, 1872, **5**, 597.
32 M. J. E. Resendiz and M. A. Garcia-Garibay, *Org. Lett.*, 2005, **7**, 371.
33 G. A. Jeffrey, *An Introduction to Hydrogen Bonding*, Oxford University Press, Oxford, 1997, pp. 39.
34 I. A. Dance, in *Encyclopedia of Supramolecular Chemistry*, ed. J. L. Atwood and J. W. Steed, CRC Press, Boca Raton, 2004, p. 1076.
35 M. Nishio, *CrystEngComm*, 2004, **6**, 130.
36 E. Weber and M. Czugler, in *Molecular Inclusion and Molecular Recognition—Clathrates II (Topics in Current Chemistry)*, ed. E. Weber, Springer-Verlag, Berlin-Heidelberg, 1988, vol. 149, p. 45.
37 I. Csöregh, S. Finge and E. Weber, *Struct. Chem.*, 2003, **14**, 241.
38 G. R. Desiraju and T. Steiner, *The Weak Hydrogen Bond (IUCr Monographs on Crystallography)*, Oxford University Press, New York, 1999, vol. 9.
39 A. L. Ringer, M. O. Sinnokrot, R. P. Lively and C. D. Sherrill, *Chem.–Eur. J.*, 2006, **12**, 3821.
40 E. Weber, in *Molecular Inclusion and Molecular Recognition—Clathrates I (Topics in Current Chemistry)*, ed. E. Weber, Springer-Verlag, Berlin-Heidelberg, 1987, vol. 140, p. 1.
41 P. N. Riley, M. G. Thorn, J. S. Vilardo, M. A. Lockwood, P. E. Fanwick and I. P. Rothwell, *Organometallics*, 1999, **18**, 3016.
42 F. H. Allen, J. A. K. Howard, W. J. Hoy, G. R. Desiraju, D. S. Reddy and C. C. Wilson, *J. Am. Chem. Soc.*, 1996, **118**, 4081.
43 J. G. Dawber and R. A. Williams, *J. Chem. Soc., Faraday Trans. 1*, 1986, **82**, 3097.
44 H. Dürr and R. Gleiter, *Angew. Chem.*, 1978, **90**, 591; H. Dürr and R. Gleiter, *Angew. Chem., Int. Ed. Engl.*, 1978, **17**, 559.
45 M. A. Beckett and J. G. Dawber, *J. Chem. Soc., Faraday Trans. 1*, 1989, **85**, 727.
46 I. Jano, *J. Chim. Phys.*, 1992, **89**, 1951.
47 M. Comes, M. D. Marcos, R. Martinez-Mánez, F. Sancenón, J. Soto, L. A. Villaescusa, P. Amorós and D. Beltrán, *Adv. Mater.*, 2004, **16**, 1783.
48 G. Bacquet, P. Bassoul, C. Combellas, J. Simon, A. Thiébault and F. Tournilhac, *Adv. Mater.*, 1990, **2**, 311.
49 J. Leonard, B. Lygo and G. Procter, *Praxis der Organischen Chemie*, VCH, Weinheim, 1996.
50 E. C. S. Jones and J. Kenner, *J. Chem. Soc.*, 1931, 1842.
51 N. J. Turro, *J. Org. Chem.*, 2002, **67**, 2606.
52 U. Kumar and T. S. Neenan, *Macromolecules*, 1995, **28**, 124.
53 A. R. Katritzky, M. Soleiman and B. Yang, *Heteroat. Chem.*, 1996, **7**, 365.
54 S. Inaba, *J. Org. Chem.*, 1985, **50**, 1373.
55 R. Ruzicka, L. Baráková and P. Klán, *J. Phys. Chem. B*, 2005, **109**, 9346.
56 R. G. Potter, *Org. Lett.*, 2007, **9**, 1187.

57 J. A. King and F. H. McMillan, *J. Am. Chem. Soc.*, 1951, **73**, 4911.
58 A. M. Roof, H. F. Van Woerden and H. Cerfontain, *J. Chem. Soc., Perkin Trans. 2*, 1979, 1545.
59 T. C. Chadwick, *Anal. Chem.*, 1974, **46**, 1326.
60 H. E. Baumgarten, *Org. Synth.*, Wiley, New York, 1973, Coll. vol. V, p. 1004.
61 R. Schröter and F. Möller, in *Methoden Org. Chem. (Houben-Weyl)*, 1957, vol. XI/1, p. 341.
62 G. M. Sheldrick, *SHELXS-97, Program for solution of crystal structures*, University of Göttingen, Germany, 1997.
63 G. M. Sheldrick, *SHELXL-97, Program for refinement of crystal structures*, University of Göttingen, Germany, 1997.
64 *CAD-4 EXPRESS*, Enraf-Nonius, Delft, The Netherlands, 1994.
65 K. Harms, *XCAD4, Program for Lp Correction of Nonius Four-Circle Diffractometer Data*, University of Marburg, Germany, 1994.